Ionospheric Threat Model Methodology for WAAS

Juan Blanch, Todd Walter, Per Enge. *Stanford University*

ABSTRACT

The ionosphere is the largest remaining error source affecting GPS. It also has some of the least predictable spatial and temporal variations. As such the ionosphere becomes the determining factor in system performance for WAAS. Because the ionosphere cannot be observed at all places simultaneously, the confidence bound, termed the Grid Ionospheric Vertical Error (GIVE), can only be determined with the aid of a threat model. The threat model is used to restrict the expected ionospheric behavior. It must not be too conservative or the resulting GIVEs will be too large and system availability will suffer. However, it must safely bound true ionospheric behavior in order to provide integrity. We therefore require a method that will accurately describe the limits without being overly pessimistic. Since the underlying physical processes driving the ionosphere are not entirely known, a decision has been made to base the threat model on reliable physical observation. There has been a long history of ionospheric observation dating back many decades. More recently, the data from the WAAS reference stations has been collected and processed to form some of the lowest noise and densest observations to date. The so-called "supertruth" data sets provide some of the most detailed observations of the ionosphere and therefore provide much of the basis for the determination of the threat model.

This paper describes a methodology for using real data to generate worst case scenarios from which an appropriate threat model may be determined. This threat model must be coupled to a set of metrics that can distinguish well-observed ionospheric regions.

INTRODUCTION

In this paper we use the standard thin shell model at a height of 350 km [1]. Instead of modeling the ionosphere as being distributed in altitude, this approximation assumes the entire electron density is in a very thin shell at a fixed height. Each ionospheric GPS measurement is represented by a location in the shell, called Ionospheric Pierce Point (IPP). The IPP is located at the intersection of the ray path going from the satellite to the reference station with the thin shell. WAAS uses these IPP measurements to form ionospheric delay estimates in a regular grid. Every point in the grid is called an Ionospheric Grid Point (IGP)[2]. These grid points are transmitted to the user who applies them to construct a location specific ionospheric correction.

Most of the time, ionospheric delay measurements that are close to each other are highly correlated; the expected vertical difference is a linear function of the separation distance[3]. In the WAAS algorithm, a local planar fit is performed to estimate the ionospheric delay for all IGP's. Unfortunately, when the ionosphere is disturbed, the spatial correlation between measurements decreases dramatically [3], so the confidence in the estimate should decrease accordingly. The WAAS algorithm solves this problem by detecting any irregularities in the ionosphere. Since the delay and confidence estimation is based on a local planar model with uncertainties bounded by a 35 cm standard deviation, an irregularity is defined as any ionospheric behavior that cannot accurately be described by such a model. The WAAS algorithm successfully detects irregularities using the chi-square consistency check or "goodness-of-fit" test. A full description of the algorithm as well as extensive validation results can be found in [4].

There is a concern, however, that some irregularities might escape detection and create integrity failures, especially at the edge of a coverage region. The following question must therefore be asnswered: How large can an irregularity be in an unobserved region, given that the chi-square does not trigger? A properly framed answer to this question would provide a threat model, taking the form of the worst case ionospheric delay as a function of a set of parameters, or metrics, describing the IPP distribution.

METHODOLOGY AND DATA USED

The problem must first be made more precise. For WAAS purposes, the two essential questions are:

- Can we have a large irregularity lying within an otherwise well behaved ionosphere? If so, how does the magnitude of the irregularity scale with its size?
- How big an irregularity can be outside a well-behaved region as a function of the distance to the observed region?

The first question corresponds to the problem of interpolating measurements, that is, we want to characterize isolated 'blobs' that could cause integrity failures. The second question corresponds to the extrapolation of measurements such that the 'strength' of ionospheric 'walls' is evaluated.

Although many of the underlying physical processes occurring during ionospheric storms are well understood [5], they do not provide quantitative limits to ionospheric behavior. As a consequence it is not possible to answer these questions with solely physical arguments. For this reason, the problem has been addressed through examination of reliable ionospheric measurements. The supertruth data provides an average of 180 measurements every 5 seconds over the Conterminous United States (CONUS) and due to the redundancy of receivers, faults have been isolated and removed [3]. Moreover, the worst ionospheric storms of the last two years have been recorded within this data. For the study presented here, the supertruth data corresponding to the ionospheric storms in the CONUS region of April 6 –7, 2000, July 15 – 16, 2000 and March 31 –April 1, 2001 were used. However, the near-storm conditions, i.e., the beginning or the end of a storm, are more likely to drive the threat model, since the worst ionospheric conditions are easily detected by the chi-square test.

The methodology used here to determine blob characteristics and wall characteristics relies on data deprivation: all the IPP's in a given region are made unavailable for the storm detectors. Thus, one obtains a simulated unobserved region of a desired shape. The general algorithm was as follows: for each IPP, exclude all IPP's within a given region and then select the IPP's needed for the planar fit among the remaining IPP's. Then perform the planar fit, apply the chi-square detector, and, in case it does not trigger, evaluate the characteristics of the unobserved region. The main characteristics are the deviation from planarity and the size of the unobserved region. The IPP's to be used for the fit were searched following the current WAAS algorithm [4]. Details concerning the planar fit can be found in [4].

BLOBS

The first goal was to see whether any narrow ionospheric disturbances could be missed if measurements were lacking where the blob occurred. Isolated blobs can take any shape, so if we wanted to test a random blob, we would have to make all possible regions invisible. However, isolated blobs can always be included in a disk such that the blob size can be conservatively described with the radius of a disk containing the blob. Without loss of generality, we can suppose blobs to be circular. As we want to systematically track any possible blob, we center the 'unobserved' disk on each IPP. For each IPP many different radii were tested.

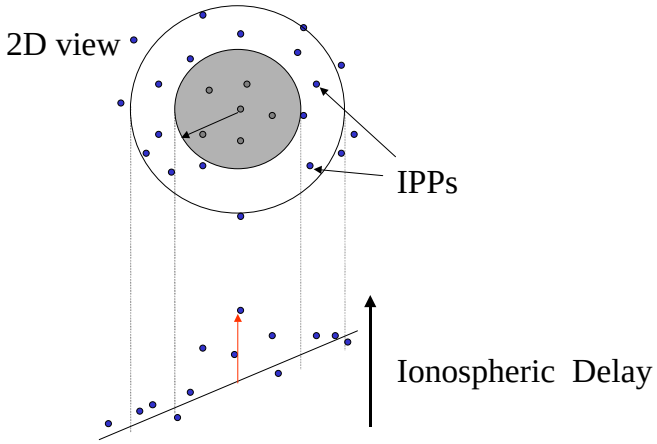

Figure 1. All IPP's in the shaded region are not considered for the fit, whereas the IPP's within the annulus were used to perform the fit.

The procedure illustrated in Figure 1 was carried out for every IPP at each radius corresponding to the exclusion of the closest IPP's. We first excluded the considered IPP. In this case the blob radius was the distance to the closest IPP. We then excluded the nearest IPP and the second nearest IPP, and the blob radius was the distance to the third IPP. Following this scheme, we excluded as many IPP's as possible. The planar fit was performed on the outer annulus. If the residuals passed the chi-square test, the maximum of the residuals inside the 'unobserved region', i.e., the blob magnitude, was computed for each IPP and each radius. The results were plotted in a two-dimensional histogram in which the height (color) of each column reflects the number of times the pair (blob radius, blob magnitude) occurs. The two dimensional histogram shown in Figure 2 was formed by testing every IPP, for every possible exclusion disk.

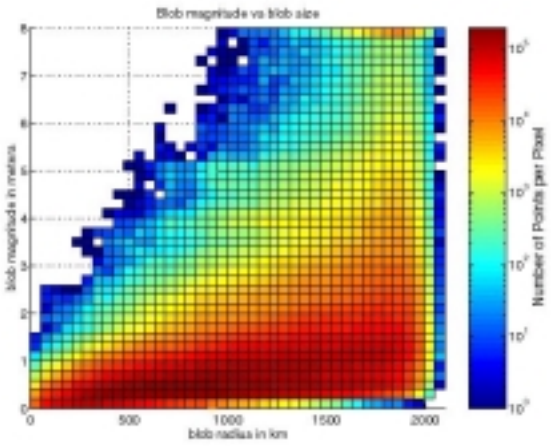

Figure 2. Two-dimensional histogram representing the distribution of the maximum deviation from planarity versus the radius of the unobserved region.

As expected, the maximum blob magnitude scales with the blob size. What is remarkable however is that for exclusion areas with radii below 500km there are no planar deviations above 5.2 m, and there are very few deviations with a magnitude above 4 meters. This result by itself shows that there are no large isolated blobs. In particular, it means that large irregularities affect a large spatial region of the ionosphere. As a consequence, the chi-square detector is very efficient.

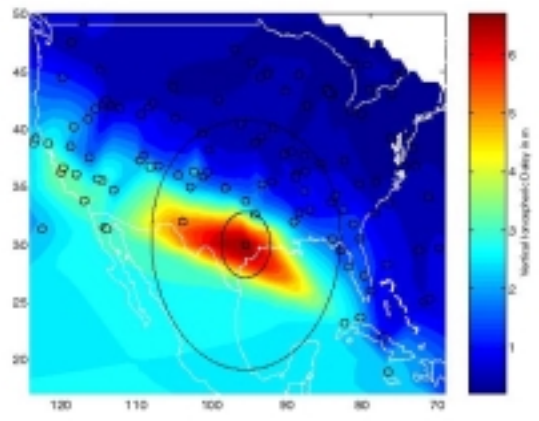

Figure 3. Worst case corresponding to a blob radius of 500 km. The true unobserved region is a half space.

The worst cases in the two dimensional histogram were examined one by one. The typical case is illustrated by Figure 3. This figure displays the IPP locations with a cubic fit in between the measurements. The small circle indicates the deprived region, and the larger one shows the radius used for the planar fit. One can observe that, although we only excluded a circular region around the IPP, the true unobserved region is significantly larger. Moreover, if one observes the previous history, we can see that the region lacking measurements at this epoch is indeed irregular. Revisiting the supertruth data we see that in the immediately preceding epochs, IPP measurements in this region appear disturbed. Consequently, this situation does not constitute a blob. Our poor coverage of IPP's has resulted in an irregularity far larger being mapped as though it applied to a 500km disk.

Maximum angle limitation

Since we want to characterize isolated regions surrounded by quiet ionosphere, we instead need to make sure that the whole region around our unobserved region is well covered. The goal was to find a parameter that describes the fact that a 'blob' is well surrounded by IPP measurements. This parameter should clearly distinguish between a well-sampled perimeter and a poorly sampled one. At the same time the parameter should be simple and easily computable. Among the several parameters analyzed, the maximum angle between adjacent IPP locations from the center of the blob best met the requirements.

The condition that the maximum angle should not exceed a given threshold was added to the condition of passing the chi-square test. Figure 4 shows the results with a threshold fixed to 80 degrees. One can see how this requirement has excluded all the worst cases. There are no blobs of a magnitude larger than 3.6 meters for a blob radius smaller than 500km; and no blobs of magnitude bigger than 4.2 meters for a blob radius smaller than 1000 km. Thus what appeared to be blobs in Figure 2 were really caused by disturbances greater than the exclusion radius.

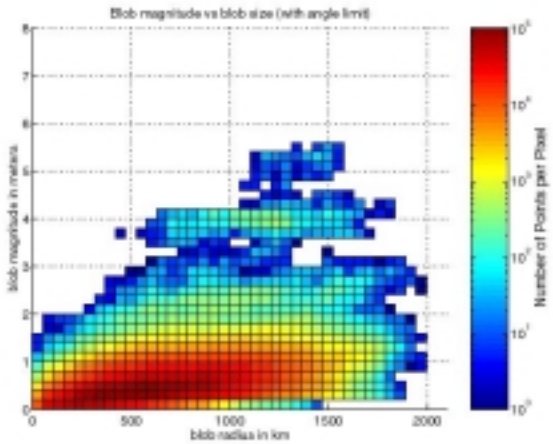

Figure 4. Two-dimensional histogram representing the distribution of the maximum deviation from planarity versus radius of the unobserved region. All IPPs for which the maximum angle between IPPs considered in the fit was larger than 80 degrees were excluded.

Fit radius

Another parameter that could play an important role in the blob size is the fit radius. It is very likely that if the quiet region surrounding the blob is larger, then the blob magnitude will be smaller. Two-dimensional histograms corresponding to different radii 800km, 1000km, 1200km, 1500km, 1800km and 2000km were generated. Figure 5 shows the peak values of such histograms, as a function of the fit radius.

Indeed, as the fit radius gets smaller the blob magnitude increases for a given blob size. Especially between 300km and 500km blob radius, the blob magnitude is 1.5 meters greater for smaller radii than for larger ones. However the blob magnitude is always below 4.5 meters for blob radii below 500km.

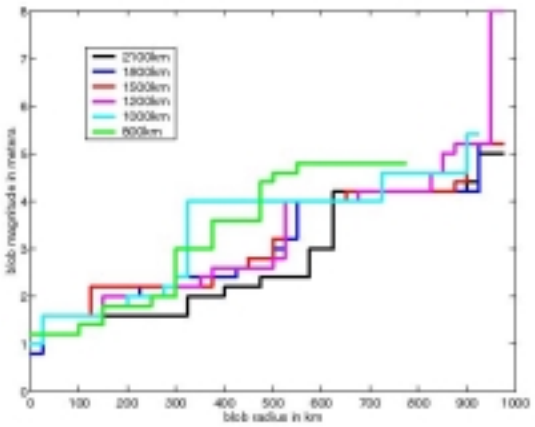

Figure 5. The different lines represent the maximum blob magnitude versus blob size for different radius of the planar fit.

Absolute magnitude versus relative magnitude

In WAAS the correction message includes the vertical ionospheric delay at each Ionospheric Grid Point and, more importantly, the confidence bound, termed the Grid Ionospheric Vertical Error (GIVE). Details on the confidence bound calculation without this threat model can be found in [4]. It takes into account :

- the decorrelation inherent to the model σ_{decorr},
- a spatial decorrelation factor that increases quadratically as we depart from the center of gravity of the IPPs
- a factor that reflects the degree of confidence we have in the model as a function of the number of points, R_{irreg}

This confidence bound reflects the formal error of the fit. We wish to determine if this formal error is sufficient to protect the user even in the presence of our data deprivation schemes. The WAAS MOPS [2] specifies the Vertical Protection Level (VPL) as being 5.33 times the 1-sigma bound in the vertical position domain. Therefore any planar deviation greater than 5.33 times the formal error could lead to an integrity failure. We formed a histogram based on the relative planar deviation, i.e. planar deviation divided by 1-sigma formal error. Figure 6 shows the two dimensional histogram of the relative deviation from planarity. There is no notable difference with its equivalent in absolute deviation: the protection is acceptable for blob sizes below 500km, but it becomes inadequate above that level.

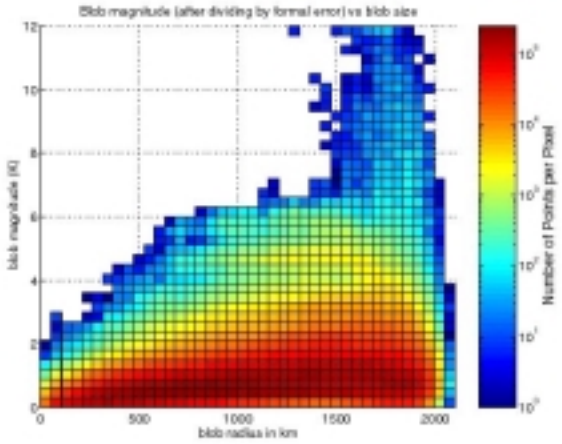

Figure 6. Two-dimensional histogram representing the distribution of the maximum relative deviation from planarity versus the radius of the unobserved region.

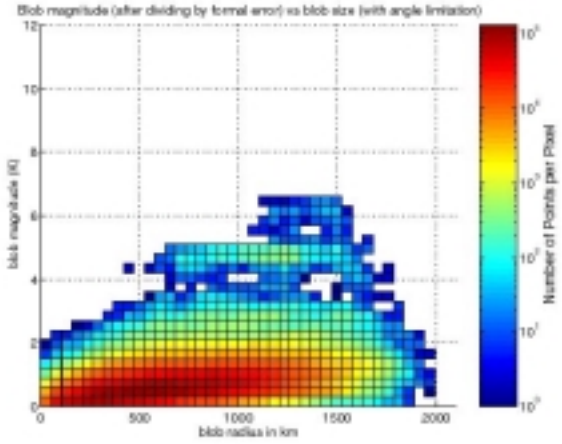

Figure 7. Two-dimensional histogram representing the distribution of the maximum relative deviation from planarity with maximum angle limitation.

Figure 7 shows that there are no relative deviations from planarity above 5.33 for blob sizes below 1000 km. This means that the formal error efficiently protects the user against blobs when the perimeter is well sampled. The results presented here strongly suggest that blobs represent a limited threat.

WALL ANALYSIS

Now we want to examine the quality of the planar fit outside the well-sampled region. Figure 8 illustrates the data deprivation scheme. The algorithm excludes all IPPs to one side of a line, performs the planar fit for the remaining IPPs, if the planar fit passes the chi-square test (meaning that the region is quiet) we compute the residuals in the unobserved region. We were interested here in the relation between the residuals and the distance to the covered region.

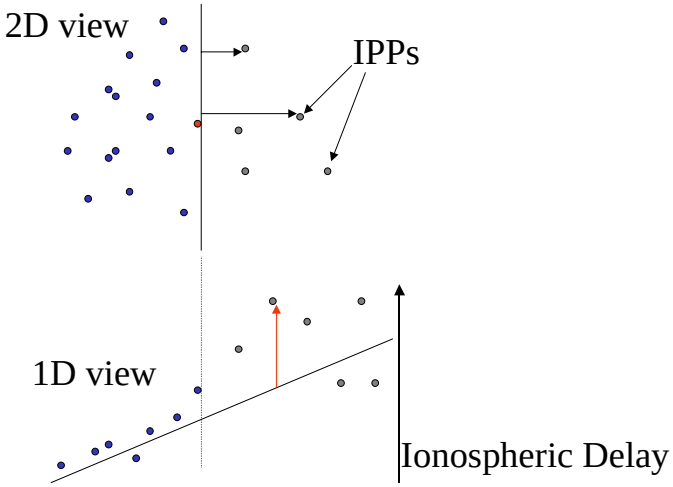

Figure 8. All IPPs to one side of the line are excluded from the planar fit.

For each IPP we computed the difference between the planar fit predicted value and the true delay as well as the distance from the IPP to the well behaved region. Two-dimensional histograms reflect the number of times the pair (distance to well-sampled region, deviation from planarity) occurs. The result of this analysis is displayed in Figure 9.

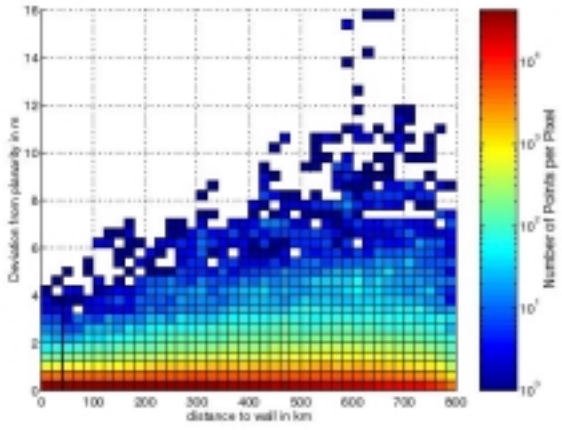

Figure 9. Two-dimensional histogram representing the deviation from planarity of the unobserved region versus the distance to the unobserved region.

As expected, the deviation from planarity increases as the distance from the observed region increases. However, the most important feature of this plot is the large value of the deviation at very small distances: 5 meters deviation is reached at only 100 km away from of a region that appears to be well sampled and quiet. One could think, following the example of blobs, that adding requirements in the observed regions, i.e., making sure that the observed region is very well sampled, could decrease the deviation from planarity at small distances. However, an examination of the worst cases persuades us that sharp separations between quiet ionosphere and disturbed ionosphere do occur. Figure 10 displays a typical worst case (here it is a 4 meters deviation at less than 50 km) and one can see that such walls may exist during ionospheric storms.

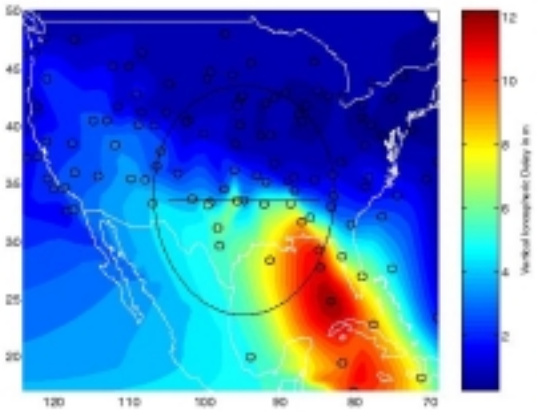

Figure 10. Sharp wall on the 16 July 2000. The region North of the straight line is quiet, whereas in the South it is disturbed.

We examined whether or not the formal error protects against such sharp walls efficiently by calculating the relative deviation from planarity instead of the absolute deviation from planarity. Figure 11 displays the resulting two dimensional histogram.

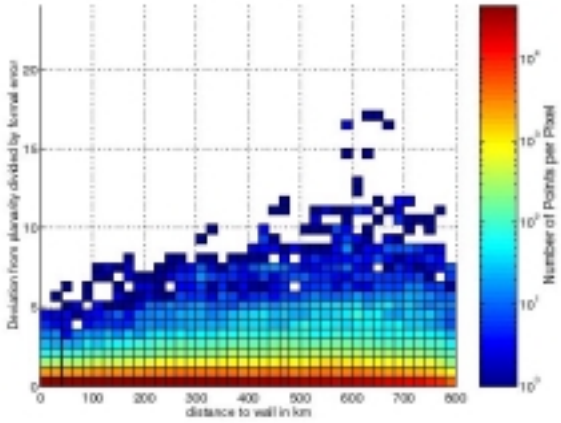

Figure 11. Two-dimensional histogram representing the relative deviation from planarity.

As in the blob analysis, the GIVE underestimates the error outside the well behaved region. This does not mean that the region outside the convex hull of the IPP's cannot be bounded, but it suggests that the GIVE has to be increased according to the distance to the covered region.

CONCLUSION

A quantitative description of the 'blob' and 'wall' threats is provided based on the supertruth data. Even in the most adverse ionosphere conditions observed to this date, irregularities within unobserved regions well surrounded by quiet ionospheric conditions can be tightly bounded. In particular, for fit radii above 800km and unobserved regions up to 500 km radius the blob magnitude rarely surpasses 4 meters.

The results of wall analysis reveal something very different: the deviation from planarity can grow very quickly outside a well-sampled region. However, a bound on the deviation from planarity as a function of the distance to the well-sampled region exists. Although the availability will be lower than for IGP's fully surrounded by quiet ionosphere, this limit can still be used to successfully produce safe confidence bounds in the edge of a coverage region.

ACKNOWLEDGEMENTS

This work was sponsored by the FAA GPS Product team (AND-730). We would also like to thank our colleagues participating in the WAAS Integrity Performance Panel (WIPP) for their guidance and numerous contributions. We thank Eric Altschuler at Raytheon and Larry Sparks, Xiaoqing Pi and Tony Manucci at JPL for providing us the supertruth data.

REFERENCES

[1] Global Positioning System Standard Positioning Service Signal Specification, June 1995.

[2]WAAS MOPS, RTCA SC 159 DO-229B.

[3] Hansen, A., Walter T., Blanch, J., and Enge, P., "Ionospheric Spatial and Temporal Correlation Analysis for WAAS," in proceedings of ION GPS, Salt Lake City, UT, September 2000.

[4] Walter, T., Hansen, A., Blanch, J. and Enge, P., "Robust Detection of Ionospheric Irregularities," in proceedings of ION GPS, Salt Lake City, UT, September 2000.

[5] Coster, Anthea J., Foster, J.C., Erickson P.J. and Rich F.J., "Regional Mapping of Storm Enhanced Density during the July 15-16 2000 Geomagnetic Storm," Proceedings of the Beacon Satellite Symposium, Boston College June 6, 2001.